PHYSICAL REVIEW B **81**, 041101(R) (2010)

Experimental demonstration of an all-optical analogue to the superradiance effect in an on-chip photonic crystal resonator system

Jun Pan,[1] Sunil Sandhu,[2] Yijie Huo,[1] Norbert Stuhrmann,[2] Michelle L. Povinelli,[3] James S. Harris,[1] M. M. Fejer,[2] and Shanhui Fan[2]

[1]*Solid State and Photonics Laboratory, Stanford University, Stanford, California 94305, USA*

[2]*E. L. Ginzton Laboratory, Stanford University, Stanford, California 94305, USA*

[3]*Ming Hsieh Department of Electrical Engineering, University of Southern California, Los Angeles, California 90089, USA*

(Received 8 December 2009; published 4 January 2010)

We show that an all-optical analogue to the Dicke superradiance effect can be observed in on-chip photonic crystal resonator systems where two resonators are separated by a distance much longer than the wavelength of the optical resonators' resonance. In addition, we provide the experimental observation of structural tuning of the superradiance effect in micron-sized optical resonators in a silicon photonic crystal slab.

DOI: 10.1103/PhysRevB.81.041101 PACS number(s): 42.60.Da, 42.60.Fc, 42.82.−m

Recent theoretical work has shown that coherence effects in atomic systems can be mapped onto on-chip microphotonic systems.[1–8] An example is the electromagnetically induced transparency (EIT) effect that has recently been observed in photonic resonator systems.[9,10] The Dicke superradiance effect,[11] where the radiation emitted by N identical neighboring atoms interfere constructively, resulting in the enhancement of the spontaneous emission rate of the system by a factor of N, has been observed using a variety of systems including atoms,[12–14] ions,[15] quantum dots,[16,17] quantum wells,[18] Josephson junctions,[19,20] and molecules in a planar microcavity.[21] Superradiance occurs when different emitters couple to a common mode of light. For photon modes that are three-dimensional in nature, the superradiance effect can only occur between emitters that were placed within about less than a wavelength of each other. All previous experiments are carried out in this regime where the emitters are placed in close proximity to one another.

In this Rapid Communication, we show that an all-optical analogue to the Dicke superradiance effect can be observed in an optical resonator system where two resonators are separated by a distance much longer than the wavelength. This is enabled by the use of a single-mode tightly confined waveguide, and the specific design that enables strong waveguide-resonator coupling. As a result, the resonators couple through a restricted one-dimensional photon continuum, which leads to the superradiance effect. In addition, we provide the first experimental observation and the structural tuning of the superradiance effect in on-chip silicon optical resonator systems. Our analysis also indicates that the presence of loss, which is inevitable in on-chip resonator systems, in fact facilitates the observation of the superradiance effect.

This work has broad implications for on-chip photonic integration, where strong waveguide-resonator coupling is essential for low loss device operation. Here, one key figure of merit is the ratio between the in-plane waveguide-resonator coupling rate and the out-of-plane radiation loss rate. Our work indicates this ratio can be enhanced through coherence effects. In addition, this result provides an indication of enforced long-distance coherence between two remotely placed resonances through the strong coupling to a common waveguide. While the present experiment is entirely a classical electromagnetic effect, one can certainly anticipate that such a coherent effect can be enforced between quantum objects (for example, two two-level systems) as well.

The origin of the superradiance effect in a photonic resonator system can be understood by considering the system shown in Fig. 1, which consists of two identical optical resonators coupled to a waveguide. There is no direct modal overlap between the resonator modes, but nevertheless, the resonators are coupled strongly through the waveguide. The system can be described by the following coupled-mode equations, which have been previously shown to accurately describe light propagation in photonic crystal resonator systems[22,23]

$$\frac{da_L}{dt} = \left(j\omega_0 - \frac{\gamma_c}{2} - \frac{\gamma_0}{2}\right)a_L + \frac{\gamma_c}{2}e^{j[\theta_2-\theta_1-\beta(\omega)L]}a_R + \sqrt{\frac{\gamma_c}{2}}e^{j\theta_1}s_{\text{in}},$$

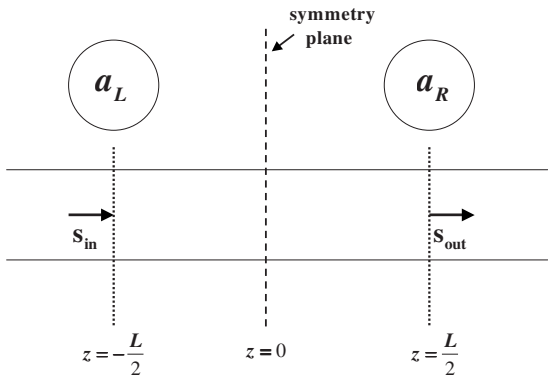

FIG. 1. A coupled resonator system that exhibits the superradiance effect. The optical resonators are identical. a_L and a_R are the modal field amplitudes in the left and right resonators, respectively, and s_{in} and s_{out} are the amplitudes of the waveguide modes incident from the left end and leaving from the right end of the waveguide, respectively.

$$\frac{da_R}{dt} = \left(j\omega_0 - \frac{\gamma_c}{2} - \frac{\gamma_0}{2}\right)a_R + \frac{\gamma_c}{2}e^{j[\theta_2-\theta_1-\beta(\omega)L]}a_L + \sqrt{\frac{\gamma_c}{2}}e^{j[\theta_2-\beta(\omega)L]}s_{\text{in}}. \quad (1)$$

Equation (1) describes the dynamics of the amplitudes of the left (right) resonator mode a_L (a_R), with the modal profile normalized such that the squared amplitude gives the energy in the mode. ω_0 is the resonant frequency of $a_{L,R}$, γ_0 is the amplitude radiative loss rate, related to the radiative quality factor as $\gamma_0=\omega_0/Q_{rad}$, γ_c is the amplitude resonator-waveguide coupling rate: $\gamma_c=\omega_0/Q_c$, the amplitude of the incoming (outgoing) wave in the waveguide is denoted by s_{in} (s_{out}) with the squared magnitude of the amplitude giving the power in the waveguide mode, $\theta_{1(2)}$ is the coupling phase associated with the forward (backward) propagating mode in the waveguide, and $\beta(\omega)$ is the waveguide dispersion relationship.

Taking into account of inversion symmetry centered at $z=0$, we can describe the system in Fig. 1 in terms of a symmetric mode $a_s=(a_L+a_R)/\sqrt{2}$ and an antisymmetric mode $a_a=(a_L-a_R)/\sqrt{2}$ using the following coupled-mode equations that are derived from Eq. (1) (Refs. 22 and 23):

$$\frac{d}{dt}\begin{Bmatrix} a_s \\ a_a \end{Bmatrix} = j\left\{\omega_0 \pm \frac{\gamma_c}{2}\sin[\phi(\omega)]\right\}\begin{Bmatrix} a_s \\ a_a \end{Bmatrix} - \left(\frac{\gamma_0}{2} + \frac{\gamma_c}{2}\{1 \pm \cos[\phi(\omega)]\}\right)\begin{Bmatrix} a_s \\ a_a \end{Bmatrix} + \sqrt{\gamma_c}e^{j[\theta_1+\theta_2-\beta(\omega)L]/2}\cos\left[\frac{\phi(\omega)}{2}\right]s_{\text{in}}, \quad (2)$$

where $\phi(\omega)=\beta(\omega)L+\theta_1+\theta_2$. From Eq. (2), the transmission through the system in Fig. 1 can be written as[22,23]

$$T(\omega) = \frac{s_{\text{out}}}{s_{\text{in}}} = 1 - \frac{\gamma_c(1-\cos[\varphi(\omega)])/2}{\gamma_0/2+\gamma_c(1-\cos[\varphi(\omega)])/2 + j(\omega_0-\gamma_c\sin[\varphi(\omega)]/2-\omega)} - \frac{\gamma_c(1+\cos[\varphi(\omega)])/2}{\gamma_0/2+\gamma_c(1+\cos[\varphi(\omega)])/2 + j(\omega_0+\gamma_c\sin[\varphi(\omega)]/2-\omega)}. \quad (3)$$

If the length L of the waveguide is chosen such that $\phi(\omega_0)$ is an odd (even) multiple of π, the antisymmetric (symmetric) mode is the superradiant mode since the radiation amplitudes into the waveguide from the two resonators constructively interfere. The symmetric (antisymmetric) mode is subradiant. As a result, if we further assume that the system is lossless (i.e., $\gamma_0=0$), the transmission spectrum $|T(\omega)|$ of the system consists of a broad dip due to a superradiant state with spontaneous emission rate enhanced by a factor of two, and an infinitesimal width peak due to a subradiant state that does not radiate.

If in addition to $\phi(\omega_0)$ being a multiple of π, a small loss is added into the resonators (i.e., $\gamma_0 \neq 0$), the subradiant state will be suppressed and the transport properties of the system will be determined solely by the superradiant state. From Eq. (3), the transmission of the system in Fig. 1 in this superradiance regime can be written as

$$T(\omega) = \frac{\gamma_0/2 + j(\omega_0-\omega)}{\gamma_0/2+\gamma_c+j(\omega_0-\omega)}. \quad (4)$$

The magnitude squared of Eq. (4) has the form of a Lorentzian dip with width $2\gamma_c$, indicating the system waveguide coupling rate enhancement due to the superradiance effect. Thus, the presence of loss, which is inevitable in on-chip resonator systems, in fact facilitates the observation of the superradiance effect.

It can be shown that the superradiance effect can also be observed for a system similar to that in Fig. 1, but with N resonators side coupled to a waveguide, provided that each resonator is separated from its neighboring resonators by a distance L such that $\phi(\omega_0)$ is a multiple of π, and a small intrinsic loss is added to each resonator. In such a system, the transmission has the form of a single Lorentzian dip with width $N\gamma_c$; this indicates a N times enhancement of the resonator-waveguide coupling rate due to the superradiance effect.[24]

We now analyze the resonator separation dependence of the superradiance effect in the system shown in Fig. 1. Figure 2 shows the analytical power-transmission spectrum and the impulse response obtained using Eq. (3) for various resonator separations L. In the plots shown in Fig. 2, the single resonator-waveguide coupling quality factor was $Q_c=4000$, the group velocity in the waveguide was $v_g=18\times10^6$ m/s, and the resonators were assumed to have a small intrinsic loss that suppresses the subradiant state. In the case of separation $L=0$ [Fig. 2(a)], the transmission spectrum shows a Lorentzian dip with a full width at half maximum $2\gamma_c$ while the impulse response shows an exponential decay rate with time constant twice as fast as the single-resonator decay rate into the waveguide, indicating the superradiance effect. When the resonator separation L is nonzero, there is a finite roundtrip delay $2L/v_g$ as the photon propagates between resonators, and, as a result, additional dips due to the Fabry-Perot effect with frequency separation $\Delta\omega/2\pi \approx v_g/2L$ are observed in the transmission spectrum [Figs. 2(b) and 2(c)]. However, as long as the frequency separation between nearby Fabry-Perot resonances satisfies $\Delta\omega > 2\gamma_c$ (or equiva-

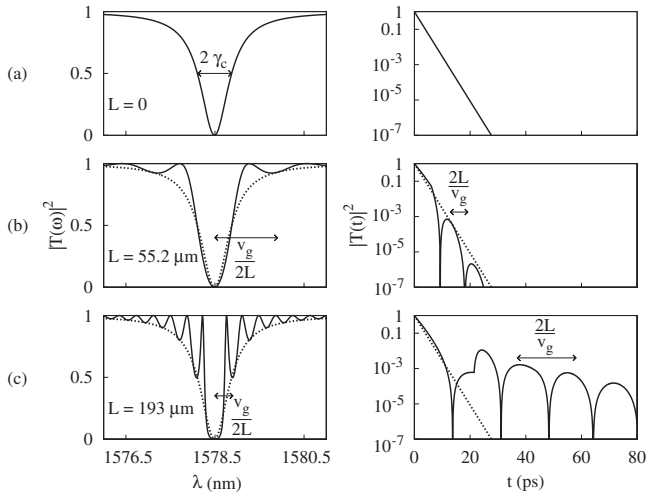

FIG. 2. Theoretical plots from coupled-mode theory showing the power-transmission spectrum (left, solid line) and the impulse response (right, solid line) for different resonator separations L in Fig. 1. Plots in (b) and (c) include the $L=0$ plots (dotted line).

lently the photon roundtrip time is greater than the lifetime $2\pi/2\gamma_c$ corresponding to the superradiant state), the center resonance dip around frequency ω_0 still has approximately twice the linewidth of a single resonance [Fig. 2(b)]. Moreover, the impulse response exhibits an exponential decay envelope with a decay rate that is twice of that of a single resonance. Thus, the superradiant state persists in this case, provided that the resonator separation satisfies

$$L < L_0 \equiv \frac{\pi v_g Q_c}{2\omega_0}. \tag{5}$$

In the opposite limit, when $L > L_0$, the frequency spacing of the Fabry-Perot resonances becomes smaller compared with the linewidth of the superradiant state [Fig. 2(c)]. The impulse response thus consists of a large number of oscillations, without an enhanced decay rate in its envelope [Fig. 2(c)]. In our experiment, the distance L_0 is estimated to be 95.1 μm. By choosing a resonator separation $L = 54.04$ μm, we are, therefore, in the superradiant regime in spite of a large separation of the two resonators by many wavelengths.

Our devices (Fig. 3) were fabricated on SOI Unibond wafers with a 1-μm buried oxide layer. The photonic crystals and strip waveguides were patterned in PMMA e-beam resist by electron beam lithography. A predeposited thin SiO_2 layer was first etched with the e-beam resist as the mask, and then served as a hard mask in transferring the pattern to the silicon layer. A 1-μm thick oxide cladding was deposited by low-pressure chemical vapor deposition and thermally annealed. Subsequently, the photonic crystal membrane was released by hydrofluoric acid, where a gold mask was used to protect the oxide cladding around the strip waveguides that couple to the photonic crystal waveguide. Inverse tapers[25] were used at the end of the strip waveguides to improve the input coupling and minimize reflections. The use of tapers substantially reduced undesirable Fabry-Perot oscillations in the transmission spectrum. Finally, the devices were cut from

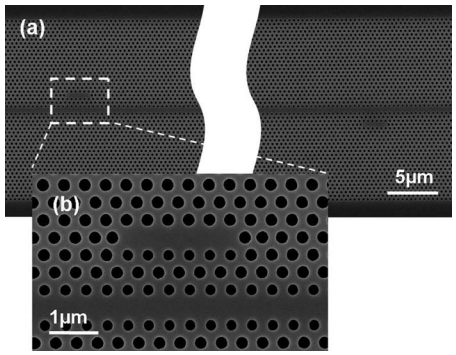

FIG. 3. Scanning electron microscope images of the fabricated device. (a) Top view of the PhC structure with two resonators. (b) Magnified view of a single resonator and a portion of waveguide.

the wafer and the facets of the waveguide were polished into mirror surfaces.

The sample that we show in Fig. 3 has two resonators with resonant frequencies in close proximity to each other. The center-to-center separation of the resonators was $L = 140a$, where $a = 386$ nm was the nearest-neighbor hole separation (lattice constant) of the structure. To measure the linewidth due to coupling between a single resonator and the

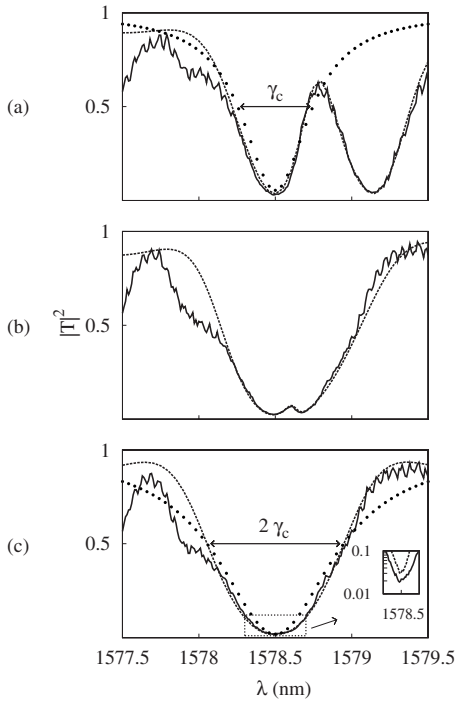

FIG. 4. Experimental power-transmission spectrum (solid line) and theoretical fits (dashed line) for the two-resonator system shown in Fig. 3 at different resonance frequency detunings between resonators: (a) $\Delta\lambda = 0.65$ nm, (b) $\Delta\lambda = 0.17$ nm, and (c) $\Delta\lambda = 0$ nm. Plots in (a) include the theoretical transmission spectrum (dotted line) of a single-resonator system with coupling rate γ_c, and plots in (c) include the theoretical transmission spectrum (dotted line) of a single-resonator system with coupling rate $2\gamma_c$. The inset of (c) shows the depth of the experimental transmission dip (solid line) is deeper compared with the depth of the single-resonator system experimental transmission dip (dashed line) from (a).

waveguide, we first detune one of the resonators using laser-pumped thermal differential tuning.[26] The output of a 514-nm Ar-ion laser was focused on the surface of the structure at a spot closer to one of the resonators than the other. The temperature rise in the vicinity of the resonator increased the refractive index and caused a redshift of its resonant wavelength. Figure 4(a) shows the transmission spectrum of the device where the detuning between the resonators was $\Delta\lambda=0.65$ nm. The theoretical fit of the full spectrum indicates a single resonator-waveguide coupling quality factor of $Q_c=4000$ and a single-resonator radiative quality factor of $Q_{\mathrm{rad}}=13,000$. The two transmission dips in Fig. 4(a) are at the resonant frequencies of the two resonators, and have widths close to the single resonator-waveguide coupling rate.

We subsequently decreased the power of the pumping laser. As the resonance frequency detuning of the two resonators is reduced, there is increased interaction between the two resonators through the waveguide [Fig. 4(b)]. Figure 4(c) shows the transmission spectrum of the device for the case when there was no frequency detuning between the two resonators. The transmission spectrum features a single transmission dip, with a lineshape closely resembling that for a waveguide coupling to a single resonator. The dip has a width corresponding to a quality factor of $Q_c=1805$, which, in comparison with the results in Fig. 4(a), indicates a nearly twofold enhancement in the resonator-waveguide coupling rate. This gives a strong indication of coherent, resonant interaction between the two resonators.

We emphasize that this coherence effect between resonators is intrinsic to the structure, and is not enforced by the use of a coherent excitation. To prove this point experimentally, we measured the transmission spectrum of the structure with a coherent laser source and with an incoherent amplified spontaneous emission (ASE) source. A comparison of the two spectrums showed that they agree well with each other, except for a small discrepancy in the maximum extinction that arises from experimental limitations when the incoherent light source was used. This agreement in the transmission spectrums indicates that the existence of the superradiant state is independent of the excitation scheme.

As an additional experimental evidence of the superradiance effect, the minimum transmission in Fig. 4(c) has a value of 0.0189, as compared to the minimum transmission value of 0.0297 in Fig. 4(a) for the single-resonance case. As can be seen from Eq. (4), the enhancement of waveguide-resonance coupling in the superradiance regime leads to a higher reduction in the forward transmission as compared to the single-resonance case.

In conclusion, we have shown that an all-optical analogue to the Dicke superradiance effect can be observed in an on-chip device using two resonators that are separated by a distance much longer than the resonance wavelength. In addition, the capability of controlling the superradiance effect using structural tuning, and the capability of observing this collective interaction using N resonators coupled to a waveguide[24] has broad implications for on-chip control of light.

This work was supported in part by the Slow Light program at DARPA DSO, under AFOSR Grant No. FA9550-05-0414.

[1] J. B. Khurgin, Phys. Rev. A **62**, 013821 (2000).
[2] D. D. Smith *et al.*, Phys. Rev. A **69**, 063804 (2004).
[3] W. Suh, Z. Wang, and S. Fan, IEEE J. Quantum Electron. **40**, 1511 (2004).
[4] L. Maleki, A. B. Matsko, A. A. Savchenkov, and V. S. Ilchenko, Opt. Lett. **29**, 626 (2004).
[5] A. B. Matsko *et al.*, J. Mod. Opt. **51**, 2515 (2004).
[6] M. F. Yanik, W. Suh, Z. Wang, and S. Fan, Phys. Rev. Lett. **93**, 233903 (2004).
[7] A. Naweed, G. Farca, S. I. Shopova, and A. T. Rosenberger, Phys. Rev. A **71**, 043804 (2005).
[8] S. F. Mingaleev, A. E. Miroshnichenko, and Y. S. Kivshar, Opt. Express **16**, 11647 (2008).
[9] Q. Xu *et al.*, Phys. Rev. Lett. **96**, 123901 (2006).
[10] X. Yang, M. Yu, D. L. Kwong, and C. W. Wong, Phys. Rev. Lett. **102**, 173902 (2009).
[11] R. H. Dicke, Phys. Rev. **93**, 99 (1954).
[12] N. Skribanowitz, I. P. Herman, J. C. MacGillivray, and M. S. Feld, Phys. Rev. Lett. **30**, 309 (1973).
[13] P. Cahuzac, H. Sontag, and P. E. Toschek, Opt. Commun. **31**, 37 (1979).
[14] C. Greiner, B. Boggs, and T. W. Mossberg, Phys. Rev. Lett. **85**, 3793 (2000).
[15] R. G. DeVoe and R. G. Brewer, Phys. Rev. Lett. **76**, 2049 (1996).
[16] X. H. Zhang *et al.*, Appl. Phys. Lett. **88**, 221903 (2006).
[17] M. Scheibner *et al.*, Nat. Phys. **3**, 106 (2007).
[18] M. Hubner *et al.*, Phys. Rev. Lett. **83**, 2841 (1999).
[19] T. F. Finnegan and S. Wahlsen, Appl. Phys. Lett. **21**, 541 (1972).
[20] K. Kobayashi and D. Stroud, Physica C **469**, 216 (2009).
[21] E. D. Angelis, F. D. Martini, and P. Mataloni, J. Opt. B: Quantum Semiclassical Opt. **2**, 149 (2000).
[22] S. Fan *et al.*, Phys. Rev. B **59**, 15882 (1999).
[23] C. Manolatou *et al.*, IEEE J. Quantum Electron. **35**, 1322 (1999).
[24] S. Sandhu, M. L. Povinelli, and S. Fan (unpublished).
[25] S. J. McNab, N. Moll, and Y. A. Vlasov, Opt. Express **11**, 2927 (2003).
[26] J. Pan *et al.*, Appl. Phys. Lett. **92**, 103114 (2008).